

Copper-catalysed synthesis of chiral alkynyl cyclopropanes using enantioconvergent radical cross-coupling of cyclopropyl halides with terminal alkynes

Received: 28 March 2024

Accepted: 30 August 2024

Published online: 26 September 2024

 Check for updates

Zeng Gao^{1,2,4}, Lin Liu^{1,3,4}, Ji-Ren Liu^{1,2}, Wang Wang^{1,2}, Ning-Yuan Yang^{1,2}, Lizhi Tao², Zhong-Liang Li², Qiang-Shuai Gu²✉ & Xin-Yuan Liu^{1,2}✉

Transition-metal-catalysed enantioconvergent cross-coupling reactions of highly reactive alkyl radicals often suffer from reduced chemoselectivity, mainly due to side reactions with closed-shell reactants. A strategy to overcome this challenge has yet to be identified, posing substantial limitations on the synthetic utility of this method. Here we report a method for enantioconvergent radical carbon–carbon cross-coupling of highly reactive cyclopropyl radicals with terminal alkynes, using redox state-tuned copper catalysis, under mild conditions. Key to this method is the use of hard chiral *N,N,N*-ligands in combination with Cu(II) salts of hard ligands/counterions, which results in elevated concentrations of Cu(II) species and thus enhanced cross-coupling reactions. This protocol not only exhibits a broad substrate scope across a wide range of both racemic cyclopropyl halide and terminal alkyne coupling partners but also provides access to useful yet synthetically challenging enantioenriched cyclopropane building blocks.

Transition-metal-catalysed C–C cross-coupling reactions are essential and widely applied methods for the expedited synthesis of complex molecular architectures¹. To this end, Fu and many others have recently made great efforts in developing chiral Earth-abundant first-row transition-metal-catalysed enantioconvergent radical cross-coupling of racemic alkyl electrophiles with assorted nucleophiles^{2–5}. By single-electron reduction, these powerful catalysts readily convert a pair of alkyl electrophile enantiomers to the same prochiral alkyl radicals, thus providing an outstanding mechanistic manifold for achieving enantioconvergence (Fig. 1a, left). Nonetheless, as the alkyl radicals become more reactive, they tend to become more susceptible to side reactions with closed-shell reactants (Fig. 1a, right),

such as coupling partners and/or chiral ligands, which are often indispensable components of the desired reaction itself. And since the desired and the side reactions all involve the common alkyl radical intermediate, the resulting diminished chemoselectivity (decreased reaction rate ratio v_1/v_2) should be independent of the alkyl radical concentration. Accordingly, the usually invoked tactics to suppress radical homocoupling side reactions by deliberately lowering the alkyl radical concentration are ineffective in this vein⁶. The only possible way to tune the chemoselectivity is to enhance the desired reaction by manipulating the Nu–Mⁿ⁺¹L* species (Nu, nucleophile; M, transition metal; L*, chiral ligand), but relevant precedents are rare in the literature⁷.

¹Shenzhen Key Laboratory of Cross-Coupling Reactions, Southern University of Science and Technology, Shenzhen, China. ²Shenzhen Grubbs Institute, Department of Chemistry, and Guangming Advanced Research Institute, Southern University of Science and Technology, Shenzhen, China. ³Department of Chemistry, Great Bay Institute for Advanced Study and Guangdong Provincial Key Laboratory of Mathematical and Neural Dynamical Systems, Great Bay University, Dongguan, China. ⁴These authors contributed equally: Zeng Gao, Lin Liu. ✉e-mail: guqs@sustech.edu.cn; liuxy3@sustech.edu.cn

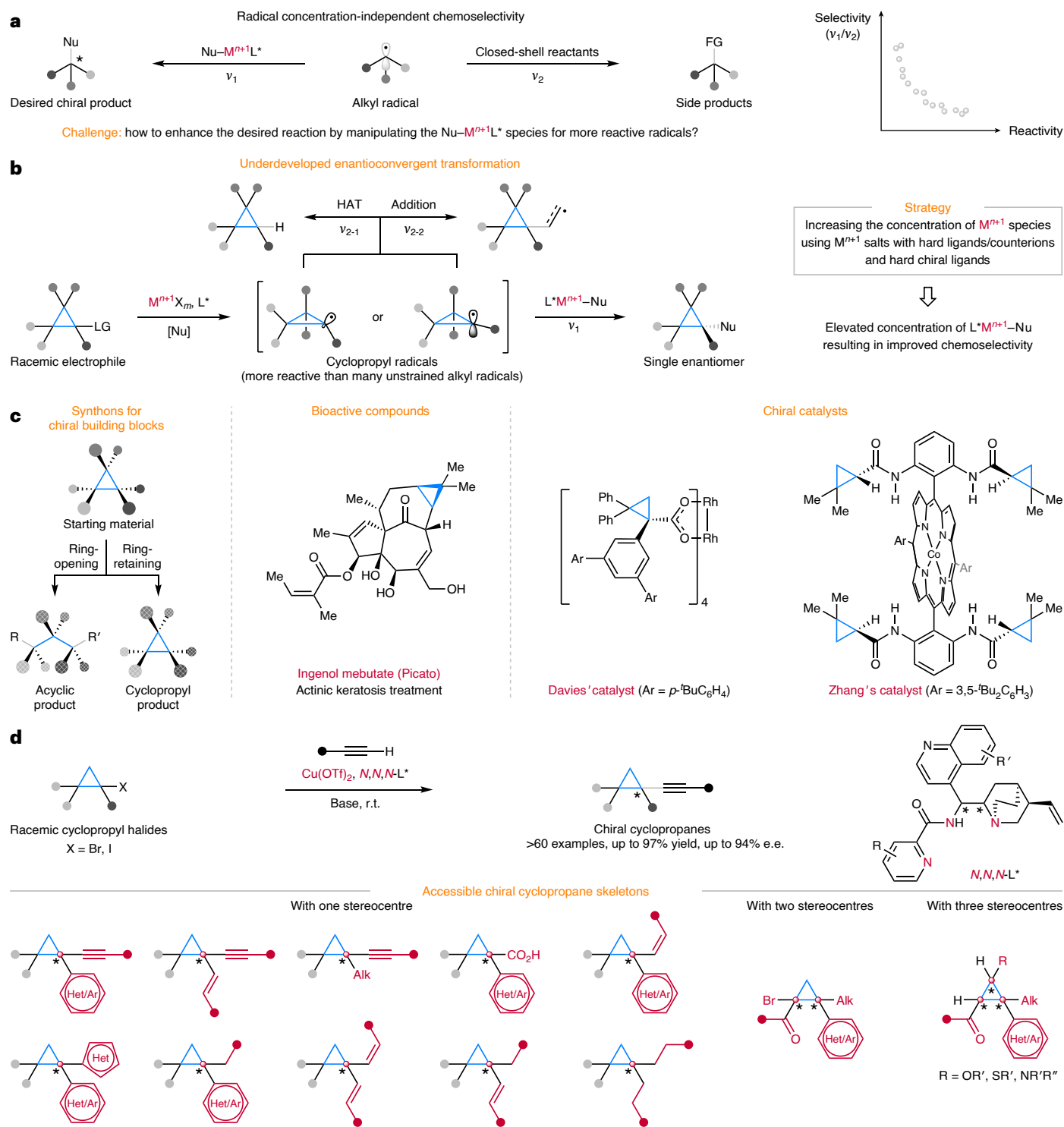


Fig. 1 | Motivation and design of enantioconvergent radical C–C cross-coupling of racemic cyclopropyl electrophiles. **a**, As radical reactivity increases, desired transition-metal-catalysed radical cross-coupling becomes more challenging due to poor chemoselectivity between it and side reactions with closed-shell reactants. **b**, This challenge is vividly illustrated by the underdeveloped transition-metal-catalysed enantioconvergent transformation of racemic cyclopropane electrophiles to enantioenriched cyclopropanes, probably as a result of the higher reactivity of cyclopropyl radicals compared with many unstrained alkyl radicals. A potential strategy to address this challenge involves increasing the concentration of M^{n+1} species using M^{n+1} catalyst precursors with hard ligands/counterions and hard chiral ligands, which would render the desired cross-coupling more competitive than side

reactions such as HAT and addition to unsaturated hydrocarbons. **c**, Chiral cyclopropanes are versatile synthetic precursors of many enantioenriched multisubstituted acyclic or cyclopropane building blocks. They are also key motifs in several natural products, drugs and catalysts. Thus, the development of transition-metal-catalysed enantioconvergent transformation of readily available racemic cyclopropyl electrophiles to enantioenriched cyclopropanes is highly desired. **d**, This work discloses an enantioconvergent radical C–C cross-coupling reaction of racemic cyclopropyl halides with terminal alkynes using redox-state-tuned copper catalysis, as mentioned above. It provides expedient access to a range of enantioenriched cyclopropane compounds featuring one to three stereocentres. v , reaction rate; FG, functional group; LG, leaving functional group; [Nu], nucleophile precursor; Het/Ar, (hetero)aryl.

This challenge can be readily appreciated in the case of cyclopropyl radicals (Fig. 1b), which are more reactive than many unstrained alkyl radicals (C–H bond dissociation energy: PhC(CH₂)₂–H, 93 kcal mol⁻¹; PhC(Me)–H, 85 kcal mol⁻¹)^{8,9}. Accordingly, the transition-metal-catalysed enantioconvergent transformations of racemic cyclopropyl electrophiles via cyclopropyl radicals have long remained underdeveloped^{10–19}, primarily due to side reactions such as hydrogen atom transfer (HAT)²⁰ and/or radical addition to unsaturated hydrocarbons²¹.

On the other hand, chiral cyclopropane rings, as the smallest carbocycles, have played a substantial role in organic synthesis. For instance, due to the manifold unique chemical reactivities imparted by the inherently high torsional and angular strains of these rings, they have served as versatile starting materials for the preparation of many chiral building blocks²² (Fig. 1c, left) and novel polymeric materials²³, and their characteristic geometries make them privileged building elements supporting a number of ligands for asymmetric transformations^{24–28} (Fig. 1c, right). In addition, chiral cyclopropanes also represent key structural moieties in a variety of natural products, pharmaceuticals, agrochemicals, fragrances and materials^{29,30} (Fig. 1c, middle). From a medicinal chemistry perspective, the introduction of a cyclopropane ring is highly likely to endow drug entities with notable pharmaceutical properties³¹, including enhanced binding, potency, metabolic stability and brain permeability, and decreased plasma clearance and off-target effects. Consequently, one such motif appears in 14 of the top 200 highest-grossing small-molecule pharmaceutical products in 2021³² and exists in more than 200 approved or currently investigated drugs³³. As such, catalytic enantioselective synthesis of enantioenriched multisubstituted cyclopropane scaffolds in a predictable and efficient manner has been recognized as a long-standing prominent objective in modern chemical research^{22,29,30,34–42}. In this regard, the main catalytic synthetic strategies at the laboratory scale and/or in industrial processes include enantioselective [2 + 1]-type cyclopropanation of acyclic starting materials^{34–39,43–49}, asymmetric transformations of prochiral cyclopropanes^{30,40} and enantioselective C–H bond functionalization of prochiral cyclopropanes^{41,42} under transition-metal catalysis, organocatalysis or enzymatic catalysis. Despite these successful methods, there have so far been relatively few reports of catalytic enantioconvergent transformations^{50,51} of racemic cyclopropanes into enantioenriched ones with high stereoselectivity^{52–54} (Fig. 1b). In addition to the aforementioned chemoselectivity issue for radical reactions, two major reasons probably account for this underdevelopment in terms of two-electron reactions. (1) Cyclopropyl cations are highly unstable species that readily undergo ring opening⁵⁵. In this respect, common cyclopropyl electrophiles, such as halides or pseudohalides, reluctantly participate in classic S_N2 reactions while their related ring-opening transformations are well reported. (2) Cyclopropyl anions, particularly corresponding organometallics, most often have good configurational stability, which prohibitively favours stereoretentive transformations^{53,56,57}. Nonetheless, the fact that racemic cyclopropanes are versatile and readily available starting materials in organic synthesis renders the development of a general catalytic system to realize such enantioconvergent transformations highly desirable because of the great potential offered by the expedited generation of densely functionalized, complex enantioenriched cyclopropanes.

Regarding cyclopropyl radical generation, a wide range of stable and highly accessible cyclopropyl electrophiles, including halides^{19,58}, carboxylic acid-derived *N*-hydroxyphthalimide esters^{59–63}, amine-derived pyridinium salts⁶⁴, and alcohols or alcohol-derived carbamothioates^{65,66}, have been reported to undergo single-electron reduction under first-row transition-metal catalysis. Accordingly, a series of non-enantioselective cyclopropane functionalization transformations have been realized to expediently access miscellaneous racemic cyclopropane compounds. Motivated by these precedents,

and based on our continued interest in copper-catalysed radical enantioconvergent cross-coupling reactions^{5,67–72}, we hypothesized that copper catalysts incorporating well-designed chiral ligands might provide an ideal platform for the development of catalytic enantioconvergent radical cross-coupling of common racemic cyclopropyl electrophiles.

To this end, we present here our efforts in developing a catalytic copper/chiral multidentate anionic *N,N,N*-ligand system to realize a general and efficient enantioconvergent radical cross-coupling of racemic cyclopropyl halides with terminal alkynes under operationally simple and mild conditions (Fig. 1d). The key to success hinges on the use of Mⁿ⁺ salts with hard ligands/counterions and hard chiral *N,N,N*-ligands to deliberately increase the concentration of Mⁿ⁺ species, thus enhancing the desired transition-metal-catalysed radical cross-coupling reaction (Fig. 1b). The reaction features broad substrate scopes (>60 examples) with respect to both coupling partners, including a broad range of racemic 1-(hetero)aryl-, 1-alkenyl- and 1-alkyl-substituted cyclopropyl halides and a variety of (hetero)aryl-, alkyl- and silyl-substituted terminal alkynes with good functional group compatibility (Fig. 1d). When combined with follow-up transformations, this reaction provides a flexible and practical platform to access a range of complex and densely functionalized enantioenriched cyclopropanes bearing one, two or even three stereocentres with most common substitution types present in useful synthetic building blocks, ligands and drugs (Fig. 1d). Given the ready availability of both coupling partners and the great potential for extension to other types of easily accessible cyclopropyl radical precursors, this work provides a complementary approach to known methods. More importantly, the redox-state tuning strategy disclosed here appears to provide a general solution to the chemoselectivity issue of highly reactive radical species, thereby facilitating the expansion of transition-metal-catalysed radical coupling reactions.

Results and discussion

Reaction development

We first investigated the enantioconvergent cross-coupling reaction of racemic 1-phenyl-2,2-dichlorocyclopropyl bromide **1** with terminal alkyne **2** (Table 1), considering that such a racemic substrate is easily available in only one synthetic step (Supplementary Fig. 1) and the chloride motif could be readily converted to many other functional groups^{19,58,73}. The desired cross-coupling product **3** was obtained in low yield, while side products **4** and **5**, probably originating from cyclopropyl radical addition to alkynes and HAT processes, respectively, were formed much more efficiently under our previously reported optimal conditions for many racemic secondary benzyl bromides (entry 1)⁶⁸. These results were expected, given the unfettered reactivity of the cyclopropyl radicals. Switching the *N,N,P*-ligand **L*1**⁷⁴ to a harder *N,N,N*-ligand **L*2** (entry 2) led to slightly better chemoselectivity (higher relative yield of **3**; see the data shown in parentheses beside the absolute yield). Consistent with this result, copper salts of hard ligands/counterions, such as acetate (entry 5) and triflate (entry 6), greatly enhanced the chemoselectivity. In contrast, those of soft ligands/counterions (entries 2–4) did not (see Supplementary Table 1 for more results). We tentatively ascribed the enhancing effect to the high predisposition of these hard ligands/counterions toward stabilizing Cu(II) species compared with the soft Cu(I) ones⁷⁵, thus increasing the concentration of chiral Cu(II) acetylide and the desired cross-coupling reaction in turn. Encouraged by these results, we were compelled to test the effect of direct use of Cu(II) salts with hard ligands/counterions and were delighted to find that both Cu(OAc)₂ (entry 7) and Cu(OTf)₂ (entry 8; Tf, trifluoromethanesulfonyl) afforded superior chemoselectivity. With the chemoselectivity issue largely resolved, we next screened several *N,N,N*-ligands (see Supplementary Table 2 for more results). Modification of the picolinamide fragment only slightly affected the enantioselectivity (**L*3**–**L*5**, entries 9–11) while replacing it with an isoquinoline carboxamide led to obviously improved enantioselectivity

Table 1 | Optimization of reaction conditions

L*1, Ar = 3,5-^tBu₂C₆H₃
L*10, Ar = 3,5-Me₂C₆H₃
L*2
L*3, R = 3-Br
L*4, R = 4-Ph
L*5, R = 5-CF₃
L*6
L*7
L*8, R, R' = ^tBu, OMe
L*9, R, R' = H, H

Entry	[Cu]	L*	Yield of 3 (%) ^a	Yield of 4 (%)	Yield of 5 (%)	e.e. of 3 (%)
1	CuTc	L*1	4 (12)	12	17	40
2	CuTc	L*2	5 (22)	10	8	-68
3	CuSCN	L*2	8 (27)	14	8	-68
4	CuI	L*2	5 (29)	6	6	-68
5	CuOAc	L*2	45 (68)	17	4	-68
6	CuOTf ₂ /2PhH	L*2	24 (68)	8	3	-68
7	Cu(OAc) ₂	L*2	44 (92)	4	ND	-68
8	Cu(OTf) ₂	L*2	44 (96)	2	ND	-68
9	Cu(OTf) ₂	L*3	28 (88)	2	2	-74
10	Cu(OTf) ₂	L*4	38 (88)	5	ND	-66
11	Cu(OTf) ₂	L*5	49 (96)	2	ND	-68
12	Cu(OTf) ₂	L*6	95 (98)	2	ND	-84
13	Cu(OTf) ₂	L*7	95 (98)	2	ND	-88
14	Cu(OTf) ₂	L*8	95 (99)	1	ND	90
15 ^b	Cu(OTf) ₂	L*8	65 (100)	ND	ND	92
16 ^{b,c}	Cu(OTf) ₂	L*8	93 (100)	ND	ND	92
17 ^{b,d}	Cu(OTf) ₂	L*8	93 (100)	ND	ND	92
18 ^{b,c,e}	Cu(OTf) ₂	L*8	61 (100)	ND	ND	92
19 ^{b,c,f}	Cu(OTf) ₂	L*8	12 (100)	ND	ND	92

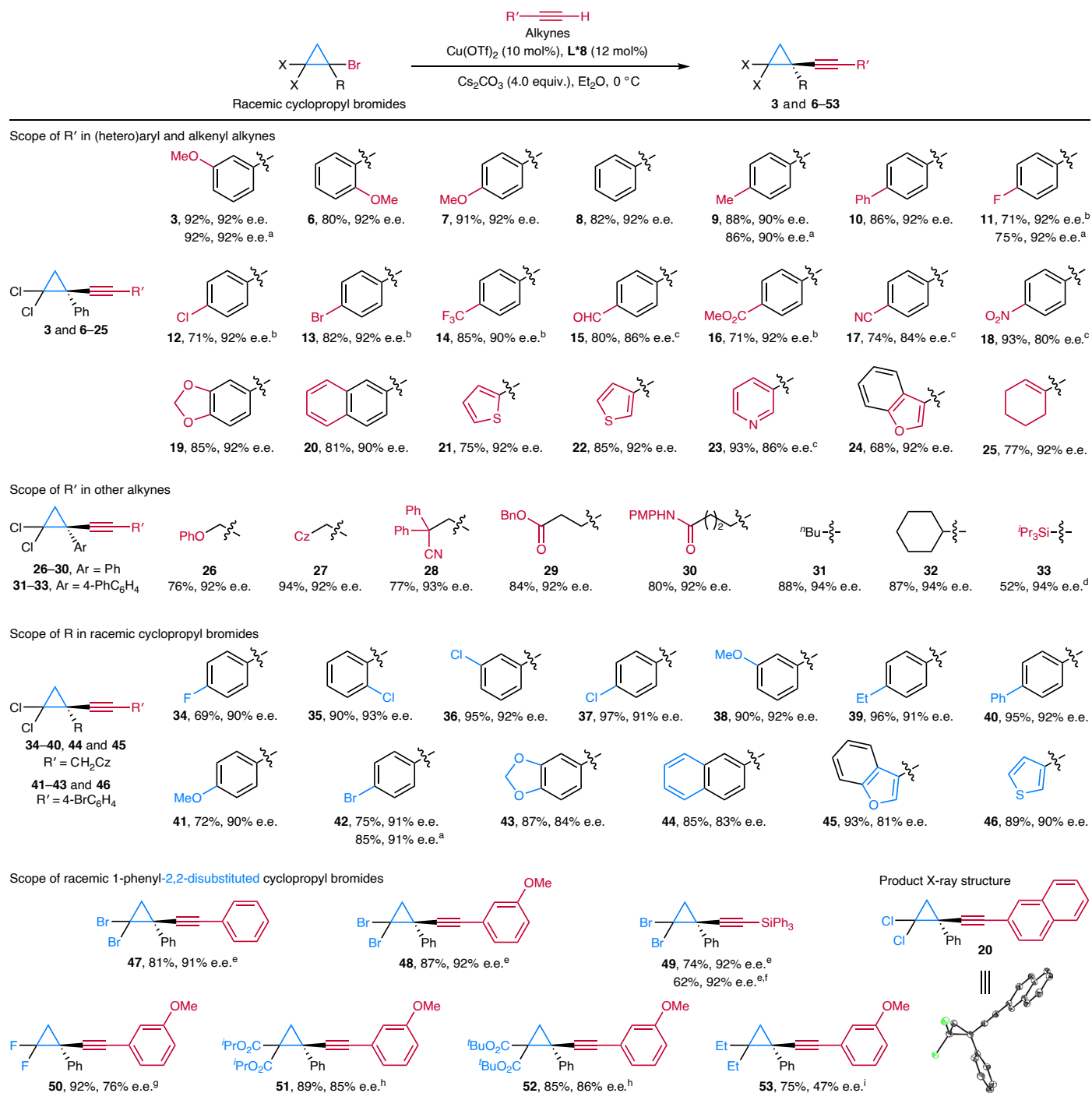
Standard reaction conditions: **2** (1.5 equiv.), racemic **1** (0.10 mmol), Cu (10 mol%), L* (12 mol%) and Cs₂CO₃ (2.0 equiv.) in diethyl ether (1.0 ml) at r.t. for 3 days under argon. Yield is based on ¹H NMR spectroscopic analysis of the crude product using 1,3,5-trimethoxybenzene as an internal standard. e.e. values are based on chiral HPLC analysis. ^aThe percentage of **3** among the three products is shown in parentheses. ^bAt 0 °C for 6 days. ^cWith **2** (1.0 equiv.), racemic **1** (0.10 mmol), Cu(OTf)₂ (15.0 mol%), L***8** (18.0 mol%) and Cs₂CO₃ (4.0 equiv.). ^dWith **2** (0.10 mmol), racemic **1** (1.5 equiv.) and Cs₂CO₃ (4.0 equiv.). ^eWith Cu(OTf)₂ (5.0 mol%) and L***8** (6.0 mol%). ^fWith Cu(OTf)₂ (2.0 mol%) and L***8** (2.4 mol%). ^tBu, *n*-butyl; ND, not determined; Ac, acetyl.

(L*6, entry 12). Introducing an *n*-butyl substituent at the C2' position of the quinoline ring (L*7, entry 13) and switching the quinine-derived chiral backbone to its (2*R*,9*R*)-pseudoenantiomer (L*8, entry 14) both modestly increased the reaction efficiency and selectivity. Lowering the reaction temperature completely suppressed the side reactions, but the yield of **3** also decreased (entry 15). Furthermore, decreasing the loading of alkyne **2** and slightly increasing the catalyst loading rescued the reaction efficiency (entry 16). The use of a slight excess of racemic electrophile **1** without altering the catalyst loading afforded almost the same results (entry 17). These results appear to indicate an inhibiting effect of alkyne on the reaction rate, as previously observed⁶⁸. As such, the optimal conditions were as follows (see Supplementary Tables 3–6 for more condition screening results): 1.0 or 1.5 equiv. racemic **1** reacted with 0.10 mmol **2** in the presence of 10 mol% or 15 mol% Cu(OTf)₂, 12 mol% or 18 mol% L***8**, and 4.0 equiv. Cs₂CO₃ in 1.0 ml diethyl ether at 0 °C under argon for 6 days, affording **3** in 93% yield with 92%

e.e. (entries 16 and 17). Lower catalyst loadings resulted in gradually decreased reaction efficiency while leaving the enantioselectivity intact (entries 18 and 19). Further control experiments confirmed that the copper salt, chiral ligand and base additive are all indispensable for the reaction (Supplementary Table 7).

Substrate scope

With the optimal reaction conditions developed, we investigated the generality of the enantioconvergent cross-coupling reaction of cyclopropyl radicals (Fig. 2). Regarding the alkyne scope, a variety of aryl alkynes bearing unsubstituted or substituted phenyl rings or a naphthalene ring successfully participated in the reaction to afford the corresponding products **3** and **6–20** in 71–93% yield with 80–92% e.e. Many common functional groups, such as methoxy (**3–7**), halo (**11–13**), trifluoromethyl (**14**), formyl (**15**), ester (**16**), cyano (**17**), nitro (**18**) and acetal (**19**), were all highly compatible with the reaction conditions.

**Fig. 2 | Substrate scopes of alkynes and racemic cyclopropyl bromides.**

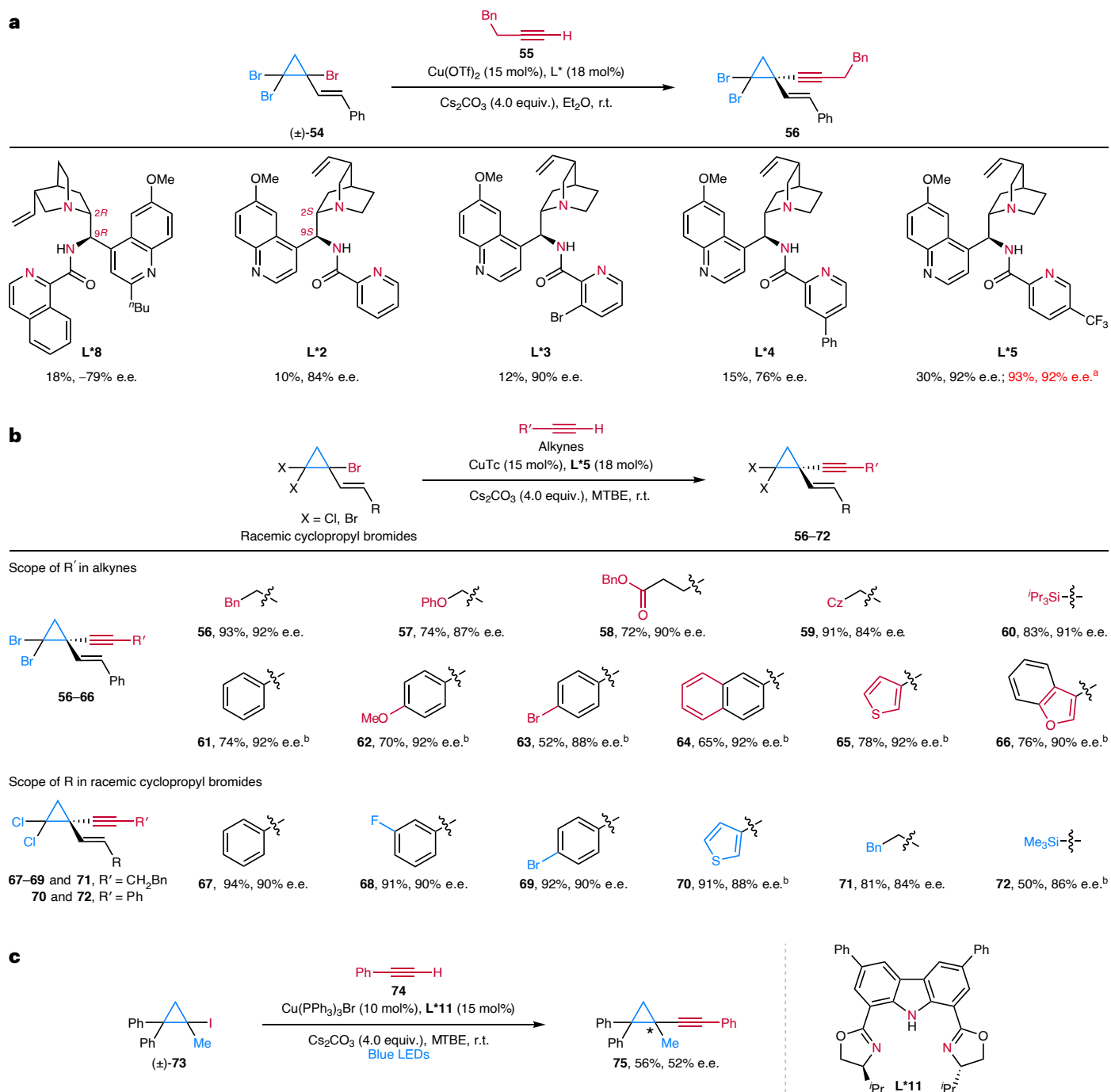
Standard reaction conditions: alkyne (0.20 mmol), racemic cyclopropyl bromide (1.5 equiv.), Cu(OTf)₂ (10 mol%), L*8 (12 mol%) and Cs₂CO₃ (4.0 equiv.) in diethyl ether (2.0 ml) under argon at 0 °C for 6 days. Isolated yield is shown; e.e. is based on chiral HPLC analysis. ^aWith alkyne (0.20 mmol), racemic cyclopropyl bromide (1.0 equiv.), Cu(OTf)₂ (15 mol%) and L*8 (18 mol%). ^bFor 8 days. ^cAt r.t. ^dWith alkyne

(0.10 mmol). ^eAt –10 °C. ^fWith triphenylsilyl acetylene (3.0 mmol). ^gWith alkyne (0.10 mmol), L*9 (12 mol%; see Table 1 for its structure) and Cs₂CO₃ (2.0 equiv.) at r.t. for 3 days. ^hWith alkyne (0.10 mmol) and L*9 (12 mol%) in PhCF₃ under blue LED irradiation (5 W) at r.t. for 3 days. ⁱWith alkyne (0.20 mmol) and L*10 (12 mol%; see Table 1 for the structure) in 1,4-dioxane under blue LED irradiation (5 W) at r.t. for 5 days. Cz, 9-carbazolyl; Bn, benzyl; PMP, 4-methoxyphenyl.

Furthermore, heteroaryl alkynes featuring medically relevant heterocycles such as thiophene (**21** and **22**), pyridine (**23**) and benzo[*b*]furan (**24**) rings were suitable substrates to give the desired products in 68–93% yield with excellent enantioselectivity. In addition, an alkenyl alkyne was also compatible with the reaction, leading to a 1,4-enyne product **25**. More importantly, a number of alkyl alkynes with different carbon chain lengths and functional groups worked well to provide

the products **26–32** in 76–94% yield with 92–94% e.e. The tolerance of carbazole (**27**) and amide (**30**) functionalities was notable. In addition, triisopropylsilyl acetylene was also applicable to the reaction to afford **33** in 94% e.e.

In terms of the scope of racemic cyclopropyl halides, a broad series of 1-aryl-substituted cyclopropyl bromides bearing 1-phenyl rings with either electron-withdrawing or electron-donating groups

**Fig. 3** Reaction development and substrate scopes for other

racemic cyclopropyl halides. a, Condition optimization for racemic 1-alkenyl-substituted cyclopropyl bromide **54**. Reaction conditions: racemic **54** (1.5 equiv.), **55** (0.050 mmol), Cu(OTf)₂ (15 mol%), L* (18 mol%) and Cs₂CO₃ (4.0 equiv.) in diethyl ether (1.0 ml) at r.t. for 4 days under argon. Yield is based on ¹H NMR spectroscopic analysis of the crude product using mesitylene as an internal standard. e.e. values are based on HPLC analysis. ^aWith CuTc (15 mol%) in MTBE (1.0 ml) for 7 days. **b**, Substrate scopes of alkynes and racemic 1-alkenyl-substituted cyclopropyl bromides. Standard reaction

conditions: racemic 1-alkenyl-substituted cyclopropyl bromide (1.5 equiv.), alkyne (0.10 mmol), CuTc (15 mol%), L*5 (18 mol%) and Cs₂CO₃ (4.0 equiv.) in MTBE (2.0 ml) at r.t. under argon for 7 days. Isolated yield is shown; e.e. is based on chiral HPLC analysis. ^bAt 10 °C for 10 days. **c**, Preliminary results of racemic 1-alkyl-substituted cyclopropyl halide **73**. Reaction conditions: racemic **73** (1.5 equiv.), phenylacetylene **74** (0.10 mmol), Cu(PPh₃)₃Br (10 mol%), L*11 (15 mol%) and Cs₂CO₃ (4.0 equiv.) in MTBE (2.0 ml) at r.t. under blue LED irradiation (5 W) and argon for 7 days.

at different positions or a naphthalene ring were all readily accommodated to give **34–44** in 69–97% yield with 83–93% e.e. In addition, 1-heteroaryl-substituted cyclopropyl bromides also underwent the reaction smoothly to afford the corresponding products **45** and **46** with good results. Remarkably, when cyclopropyl bromides served

as the limiting reagents, products **3**, **9**, **11** and **42** were obtained in similar yields with identical enantioselectivity under the alternative optimal conditions (Table 1, entry 16), making these conditions preferable for less accessible electrophile substrates. More importantly, 2,2-dibromocyclopropyl bromides were also viable substrates to give

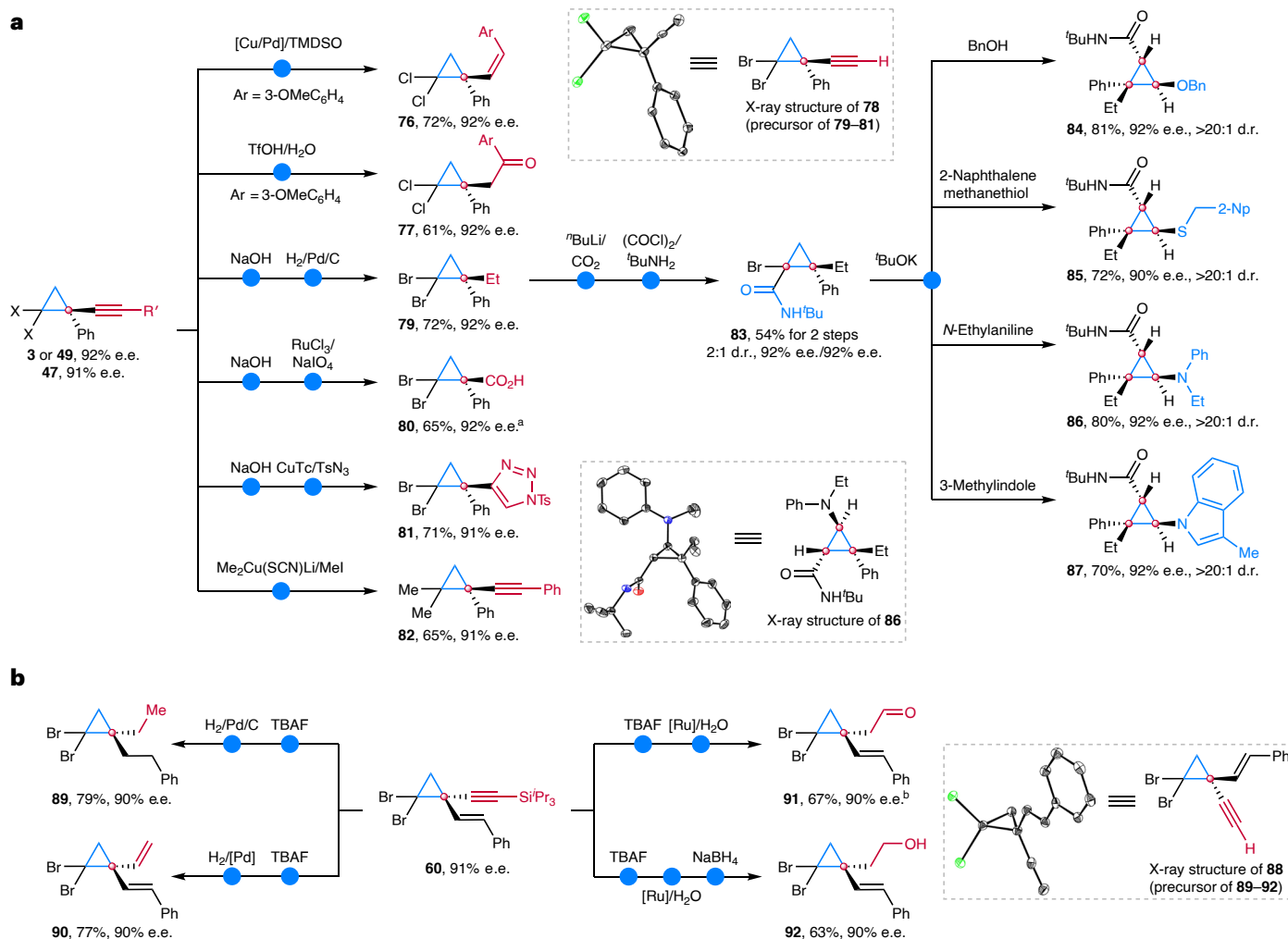


Fig. 4 | Synthetic utility for the construction of valuable enantioenriched cyclopropane building blocks. a, Transformations of 1-phenyl-substituted cyclopropanes. **b**, Transformations of 1-alkenyl-substituted cyclopropanes. ^aThe e.e. value of **80** was deduced from that of its methyl ester derivative. ^bThe e.e. value of **91** was deduced from that of **92**. [Cu/Pd], [1,3-bis[2,6-bis(1-methylethyl)

phenyl]-2-imidazolidinylidene]chlorocopper/palladium acetate/dicyclohexyl(2'-methoxy[1,1'-biphenyl]-2-yl)phosphine; TMSO, 1,1,3,3-tetramethyldisiloxane; Ts, *para*-toluenesulfonyl; 2-Np, 2-naphthyl; TBAF, tetra-*n*-butylammonium fluoride; [Ru], tris(acetonitrile)(η^5 -cyclopentadienyl) ruthenium hexafluorophosphate; [Pd], Lindlar catalyst.

the corresponding products **47–49** with good yield and excellent enantioselectivity. In particular, the reaction leading to **49** on the gram scale proceeded well without any apparent loss of enantioselectivity. In addition, the reaction of 2,2-difluorocyclopropyl bromides proceeded smoothly under slightly modified conditions, yielding the corresponding products **50** in excellent yield with good enantioselectivity. By contrast, 2,2-dialkoxycarbonyl and 2,2-dialkyl cyclopropyl bromides (see Supplementary Tables 8 and 9 for information on the condition optimization of the 2,2-dialkyl substrate) required light irradiation for efficient reaction initiation. This is probably due to the substantially increased steric hindrance and diminished electron-withdrawing inductive effects, which retard the reduction of these compounds. Nonetheless, the desired products **51–53** were efficiently obtained in high or promising enantiopurity (see Supplementary Fig. 2 for results of **50–52** under the standard conditions). Unfortunately, 2,2-diphenyl cyclopropyl bromides underwent exclusive ring-opening side reactions⁷⁶, providing no desired products (Supplementary Fig. 2).

To further demonstrate the utility of this method, we examined the cross-coupling of racemic 1-alkenyl-substituted cyclopropyl bromides to access enantioenriched cyclopropyl-tethered 1,4-enynes, which are an important class of versatile synthons because both the alkenyl and alkynyl groups are highly transformable⁷⁷. The

enantioconvergent cross-coupling reaction of racemic 1-alkenyl-2,2-dibromocyclopropyl bromide **54** with terminal alkyne **55** was first investigated (Fig. 3a). Unfortunately, the originally superior ligand **L*8** for racemic 1-(hetero)aryl-substituted cyclopropyl bromides showed low reaction efficiency with unsatisfactory enantioselectivity (18% yield and -79% e.e. for **56**; Fig. 3a and Supplementary Table 10, entry 2). Accordingly, we first re-examined the chiral ligands and found that **L*5** provided both enhanced reaction yield and outstanding enantioselectivity (Fig. 3a and Supplementary Table 10, entries 3–6). Subsequent screening of copper salts and solvents revealed copper(I) thiophene-2-carboxylate (CuTc) and methyl *tert*-butyl ether (MTBE) as the superior combination (Supplementary Table 10, entries 7–11). Notably, using a Cu(I) precatalyst did not result in side reactions for the 1-alkenyl cyclopropyl bromide, probably indicating a higher stability of the corresponding 1-alkenyl cyclopropyl radical than those from 1-aryl cyclopropyl halides. Consequently, the optimal conditions were identified as follows (Fig. 3a and Supplementary Table 10, entry 12): the reaction of racemic **54** (1.5 equiv.) and **55** (0.050 mmol, 1.0 equiv.) in the presence of CuTc (15 mol%), **L*5** (18 mol%) and Cs₂CO₃ (4.0 equiv.) in MTBE (1.0 ml) at r.t. under argon for 7 days delivered **56** in 93% yield with 92% e.e. Under these conditions, various alkyl-, silyl- and (hetero)aryl-substituted alkynes were successfully coupled

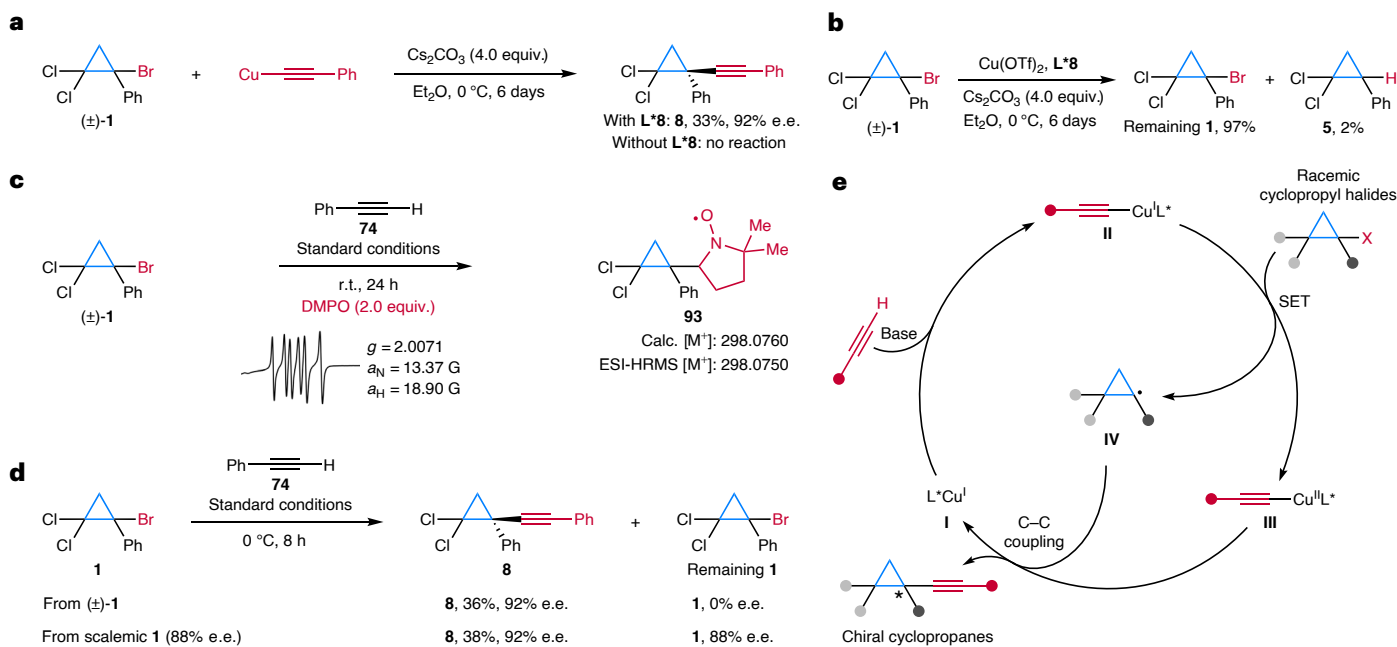


Fig. 5 | Mechanistic studies and proposals. **a**, Copper phenylacetylide directly participated in the reaction in the presence of ligand **L*8**. **b**, Radicals were hardly generated under the standard conditions in the absence of alkyne. **c**, The EPR and electro spray ionization (ESI) HRMS experimental results indicated the formation of DMPPO-trapped product **93**, supporting the cyclopropyl radical generation. **d**, Racemic and scalemic **1** provided product **8** with the same enantioselectivity,

and the recovered starting materials indicated no enantioenrichment or enantioerosion, evidencing an enantioselective stereoablative process. Values aligned horizontally belong to one experiment. **e**, The reaction was proposed to proceed via SET between the in situ-generated copper acetylide complexes **II** and racemic cyclopropyl halides to form Cu(II) complexes **III** and cyclopropyl radical **IV** and their subsequent enantioselective C–C bond coupling.

with **54** to give **56–66** in 52–93% yield with 84–92% e.e. (Fig. 3b). Furthermore, (hetero)aryl-, alkyl- and silyl-substituted 1-alkenyl cyclopropyl bromides were suitable substrates for this reaction to give **67–72** in excellent yield with good enantioselectivity.

Motivated by the aforementioned success, we proceeded to explore the coupling of 1-alkyl cyclopropyl iodide **73** (Fig. 3c). This substrate presents additional difficulty because of its more challenging single-electron reduction and the increased reactivity of the resulting cyclopropyl radicals due to the absence of conjugation with α -substituents. Indeed, the optimized copper catalysts with **L*8** and **L*5** for 1-(hetero)aryl and 1-alkenyl cyclopropyl bromides both failed to reduce **73** (Supplementary Table 11, entries 1 and 2) under the corresponding thermal conditions, respectively. Photoexcited copper acetylide complexes were reported to possess much stronger reducing capability than ground-state copper complexes^{78,79}. Thus, we investigated a series of electron-rich tridentate anionic ligands under blue light-emitting diode (LED) irradiation (Supplementary Table 11). Interestingly, ligand **L*11**⁸⁰ performed the best to give the desired product **75** in moderate yield with promising enantioselectivity (Fig. 3c and Supplementary Table 11, entry 6). The reaction conditions are currently being further optimized in our laboratory.

Synthetic utility

Considering that both the halide and alkyne functionalities in the thus-obtained products are highly transformable in organic synthesis, we envisioned a general and practical platform based on this enantioconvergent cross-coupling process for the rapid construction of a wide range of valuable enantioenriched cyclopropane building blocks (Fig. 4). Accordingly, we first converted the alkyne moiety in **3** to a Z-alkenyl group in **76** or a carbonyl group in **77** (Fig. 4a). In addition, the triphenylsilyl group in **49** was easily removed to provide the terminal alkyne **78**, which subsequently underwent complete hydrogenation, oxidative cleavage or copper-catalysed azide–alkyne

cycloaddition reactions to afford alkane **79**, carboxylic acid **80** or 1,2,3-triazole **81**, respectively. Regarding the halide functionalities, direct substitution⁸¹ of the dibromo groups in **47** with dimethyl groups was readily achieved to afford 2,2-dialkyl cyclopropane **82**. Additionally, monolithiation of **79** followed by trapping with CO₂ and further amidation led to **83** in moderate diastereoselectivity. More importantly, the subsequent highly diastereoselective formal nucleophilic substitution⁷³, consisting of sequential HBr elimination and conjugate nucleophile addition, readily transformed the diastereomeric mixture of **83** into multisubstituted cyclopropane derivatives **84–87** featuring three contiguous stereogenic carbons. As for the alkyne group in **60**, straightforward desilylation delivered the terminal alkyne **88**, of which the following partial hydrogenation, hydration, or sequential hydration and reduction provided diene **90**, aldehyde **91** or alcohol **92**, respectively (Fig. 4b). In addition, the alkenyl group in **60** is also of high synthetic potential. For example, complete hydrogenation of **88** gave rise to the *gem*-dialkyl-substituted cyclopropane **89**. Notably, the current synthetic protocols allowed facile access to enantioenriched alkyl-substituted cyclopropanes, such as **77**, **79**, **89** and **91**, thus providing an excellent complementary approach to the direct yet currently underdeveloped enantioselective cross-coupling of 1-alkyl-substituted cyclopropyl halides (Fig. 3c). Importantly, no apparent loss of enantioselectivity was observed in all the above transformations, showcasing the high adaptability and practicability of this method toward various enantioenriched cyclopropane building blocks. The absolute configurations of **20** (Fig. 2 and Supplementary Fig. 3), **78** (Fig. 4 and Supplementary Fig. 4), **86** (Fig. 4 and Supplementary Fig. 5) and **88** (Fig. 4 and Supplementary Fig. 6) were determined by X-ray crystallographic analysis, and those of all related other compounds were assigned by analogy.

Mechanistic considerations

First, the reaction of stoichiometric copper acetylide with racemic **1** afforded product **8** with 92% e.e. in the presence of **L*8**, but

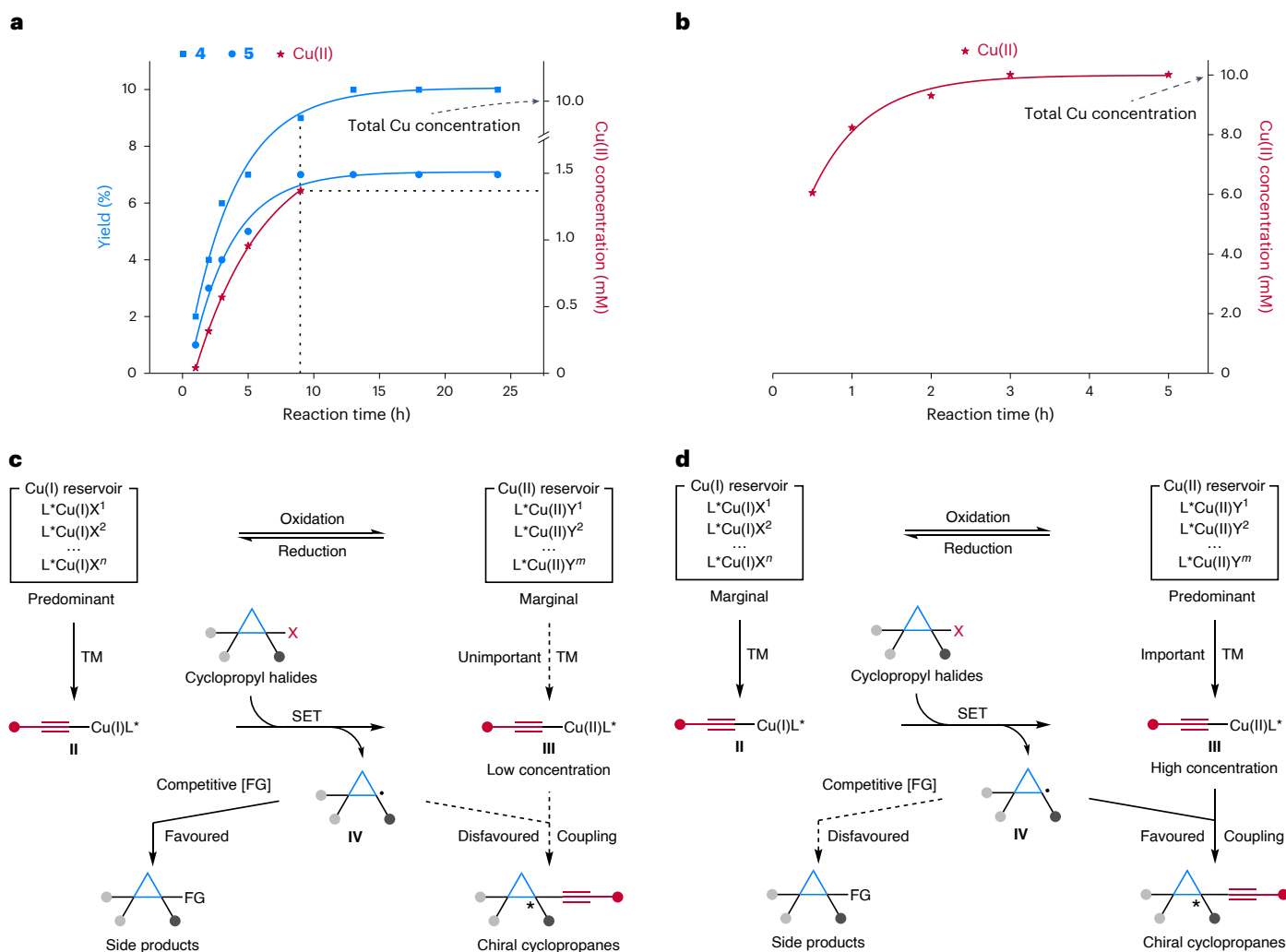


Fig. 6 | Preliminary experimental results and rationale for redox-state-tuned copper catalysis. **a**, Time-course experiments revealed the gradual build-up of Cu(II) species, as indicated by EPR spectroscopy, when CuOTf was used as the catalyst precursor. This process was accompanied by enhanced suppression of side products. **b**, The use of Cu(OTf)₂ as a precatalyst resulted in a much higher concentration of Cu(II) species, accompanied by the complete suppression of side reactions. The solid lines represent exponential decay fits to the experimental data. **c**, Under conditions with high Cu(I)/Cu(II) ratios, the

formation of Cu(II) acetylide **III** primarily relies on the single-electron oxidation of **II** by cyclopropyl halides. Consequently, the concentration of **III** is low, making its coupling with cyclopropyl radicals unfavourable and leading to the formation of side products. **d**, Under conditions with low Cu(I)/Cu(II) ratios, the transmetalation of Cu(II) species leading to **III** can substantially increase the concentration of **III**, thus favouring the desired radical coupling and suppressing side reactions. TM, transmetalation.

no reaction occurred without **L*8**. These results indicated that the ligand-coordinated copper(I) acetylide might work as the key species to promote the reaction initiation and product formation (Fig. 5a). Second, a control experiment without alkyne showed essentially no conversion of **1**, further supporting the involvement of copper(I) acetylide in the electrophile reduction (Fig. 5b). Third, electron paramagnetic resonance (EPR) and high-resolution mass spectrometry (HRMS) analysis of the reaction mixture with **1** in the presence of the radical trap 5,5-dimethyl-1-pyrroline *N*-oxide (DMPO) collectively revealed the formation of DMPO-trapped product **93** (Fig. 5c and Supplementary Fig. 7). In addition, the reaction was completely shut down in the presence of a radical inhibitor TEMPO (Supplementary Fig. 8). Collectively, these results supported the generation of cyclopropyl radicals in the reaction. Fourth, the reactions with either racemic or scalemic **1** afforded product **8** with the same enantioselectivity. Furthermore, no enantioenrichment or enantioerosion of recovered **1** was observed when racemic or scalemic **1**, respectively, was used (Fig. 5d; see Supplementary Fig. 9 for similar results of **73**). These results together excluded

the involvement of kinetic resolution or fast racemization of cyclopropyl bromides in the reaction. On the basis of the above results and our previous reports^{68,69}, a possible mechanism was proposed, as shown in Fig. 5e. Initially, L^{*}Cu(I) intermediate **I** reacted with terminal alkynes in the presence of a base to generate the L^{*}Cu(I)–acetylide intermediate **II**. Afterwards, intermediate **II** underwent single-electron transfer (SET) with racemic cyclopropyl halides, giving rise to the L^{*}Cu(II)–acetylide intermediate **III** and cyclopropyl radical **IV**. Finally, the enantioselective C–C bond coupling occurred via the reaction of **III** and **IV**, forging the enantioenriched cyclopropane products and regenerating the L^{*}Cu(I) (**I**) catalyst. Our preliminary theoretical investigations into this C–C bond formation step suggested a likely radical substitution-type pathway, which is approximately 3.2 kcal mol^{−1} more favourable than the pathway involving Cu(III) species formation and subsequent reductive elimination (Supplementary Figs. 14–17 and Supplementary Table 13).

Regarding the redox-state-tuning, we investigated the impact of mixed catalyst precursors of Cu(I) and Cu(II) and observed an increase in the formation of side products when Cu(I) was predominant

(Supplementary Table 12). Importantly, detailed time-course experiments with a Cu(I) catalyst precursor revealed that the formation of side products plateaued (Fig. 6a and Supplementary Fig. 10) after the overall concentration of Cu(II) species increased to approximately 1.5 mM at around 9 h (Fig. 6a), as indicated by EPR experiments (Supplementary Figs. 11 and 13). Additionally, the use of a Cu(II) catalyst precursor resulted in an almost order of magnitude higher concentration of Cu(II) species (Fig. 6b and Supplementary Figs. 10, 12 and 13), and the side reactions were completely suppressed. These results clearly demonstrated a chemoselectivity change depending on the concentration of Cu(II) species.

We rationalized this Cu(II)-promoted chemoselectivity by referring to the stoichiometric Cu(II)-promoted Sandmeyer hydroxylation reaction⁸² and copper-mediated reversible-deactivation radical polymerization⁸³. In these reaction systems, the increased Cu(II) species concentration directly or indirectly raises the concentration of LCu(II)-OH or LCu(II)-halide, thus favouring their coupling reactions with aryl or alkyl radicals. Accordingly, the chemoselectivity shifts from hydrogen atom abstraction or radical propagation toward hydroxylation or deactivation, respectively, and the deliberate control of Cu(II) species concentration proves to be essential for achieving high reaction efficiency or reduced polymer polydispersity.

Similarly, in our reaction, the Cu(II) and Cu(I) species are believed to dynamically interconvert through redox processes^{84,85}, with their relative ratios depending on specific reaction conditions (Table 1 and Fig. 6a,b). Under conditions where Cu(I) species are predominant and Cu(II) species are marginal (Fig. 6c), the formation of Cu(II) acetylide **III** mainly relies on the single-electron oxidation of **II** by cyclopropyl halides. Consequently, the concentration of **III** is greatly limited, and its coupling with cyclopropyl radicals is outcompeted by other reactants. Conversely, under conditions with a high proportion of Cu(II) species (Fig. 6d), their direct transmetalation⁸⁶ leading to **III** can be pronounced, thereby greatly increasing the concentration of **III** and favouring the desired radical coupling. Overall, these findings underscore the importance of redox-state-tuned copper catalysis in enhancing the chemoselectivity of highly reactive cyclopropyl radicals.

Summary

We have established a method for the enantioconvergent radical carbon-carbon cross-coupling of abundant racemic cyclopropyl halides with a wide range of terminal alkynes, under mild conditions. The success of the approach hinges largely on the redox-state-tuning of copper catalysts, achieved by employing Cu(II) catalyst precursors with hard ligands/counterions in conjunction with hard chiral *N,N,N*-ligands. Further transformations of the coupling products rapidly generate a broad library of valuable enantioenriched cyclopropanes characterized by over ten distinct types of substitution patterns with up to three contiguous stereocentres, showcasing the potential of this method for the assembly of a diverse range of synthetically challenging enantioenriched cyclopropanes present in synthetic building blocks, ligands and drugs. We anticipate that this strategy will spur the development of more enantioconvergent cross-coupling reactions of highly reactive alkyl radicals with distinct types of nucleophiles.

Methods

Representative procedure for 1-(hetero)aryl cyclopropyl bromides

An oven-dried resealable Schlenk tube equipped with a magnetic stir bar was charged with Cu(OTf)₂ (7.20 mg, 0.020 mmol, 10 mol%), chiral ligand **L*8** (12.80 mg, 0.024 mmol, 12 mol%) and Cs₂CO₃ (256.0 mg, 0.80 mmol, 4.0 equiv.). The tube was evacuated and backfilled with argon three times. Then, racemic 1-(hetero)aryl cyclopropyl bromide (0.30 mmol, 1.5 equiv.), alkyne (0.20 mmol, 1.0 equiv.) and diethyl ether (2.0 ml) were sequentially added into the mixture under argon. The tube was sealed, and the reaction mixture was allowed to stir at 0 °C

for 6 days. Upon completion of the reaction (monitored by thin-layer chromatography (TLC)), the mixture was then filtered through a pad of celite and rinsed with ethyl acetate. The filtrate was evaporated, and the residue was purified by column chromatography on silica gel to afford the desired product.

Representative procedure for 1-alkenyl cyclopropyl bromides

An oven-dried resealable Schlenk tube equipped with a magnetic stir bar was charged with CuTc (2.85 mg, 0.015 mmol, 15 mol%), **L*5** (8.90 mg, 0.018 mmol, 18 mol%) and Cs₂CO₃ (128.0 mg, 0.4 mmol, 4 equiv.). The tube was evacuated and backfilled with argon three times. Then, racemic 1-alkenyl cyclopropyl bromide (0.15 mmol, 1.5 equiv.), alkyne (0.10 mmol, 1.0 equiv.) and MTBE (2.0 ml) were sequentially added into the mixture under argon. The tube was sealed, and the reaction mixture was allowed to stir at r.t. for 7 days. Upon completion of the reaction (monitored by TLC), the mixture was filtered through a pad of celite and rinsed with ethyl acetate. The filtrate was evaporated, and the residue was purified by column chromatography on silica gel to afford the desired product.

Representative procedure for 1-alkyl cyclopropyl bromides

An oven-dried resealable Schlenk tube equipped with a magnetic stir bar was charged with Cu(PPh₃)₃Br (9.30 mg, 0.010 mmol, 10 mol%), **L*11** (8.12 mg, 0.015 mmol, 15 mol%) and Cs₂CO₃ (128.0 mg, 0.4 mmol, 4 equiv.). The tube was evacuated and backfilled with argon three times. Then, racemic 1-alkyl cyclopropyl iodine **73** (50.1 mg, 0.15 mmol, 1.5 equiv.), alkyne **74** (0.10 mmol, 1.0 equiv.) and MTBE (2.0 ml) were sequentially added into the mixture under argon. The tube was sealed, and the reaction mixture was stirred under blue LED irradiation (5 W) at r.t. for 7 days. Upon completion of the reaction (monitored by TLC), the mixture was filtered through a pad of celite and rinsed with ethyl acetate. The filtrate was evaporated, and the residue was purified by column chromatography on silica gel to afford the desired product.

Data availability

All data are available in the main text and Supplementary Information. Crystallographic data for the structures reported in this article have been deposited at the Cambridge Crystallographic Data Centre, under deposition numbers CCDC 2264730 (**20**), 2267172 (**78**), 2267173 (**86**) and 2264731 (**88**). Copies of the data can be obtained free of charge at <https://www.ccdc.cam.ac.uk/structures/>.

References

- de Meijere, A., Bräse, S. & Oestreich, M. (eds) *Metal-Catalyzed Cross-Coupling Reactions and More* (Wiley, 2014).
- Choi, J. & Fu, G. C. Transition metal-catalyzed alkyl-alkyl bond formation: another dimension in cross-coupling chemistry. *Science* **356**, eaaf7230 (2017).
- Fu, G. C. Transition-metal catalysis of nucleophilic substitution reactions: a radical alternative to S_N1 and S_N2 processes. *ACS Cent. Sci.* **3**, 692–700 (2017).
- Cherney, A. H., Kadunce, N. T. & Reisman, S. E. Enantioselective and enantiospecific transition-metal-catalyzed cross-coupling reactions of organometallic reagents to construct C–C bonds. *Chem. Rev.* **115**, 9587–9652 (2015).
- Dong, X.-Y., Li, Z.-L., Gu, Q.-S. & Liu, X.-Y. Ligand development for copper-catalyzed enantioconvergent radical cross-coupling of racemic alkyl halides. *J. Am. Chem. Soc.* **144**, 17319–17329 (2022).
- Leifert, D. & Studer, A. The persistent radical effect in organic synthesis. *Angew. Chem. Int. Ed.* **59**, 74–108 (2020).
- Hanson, P., Rowell, S. C., Walton, P. H. & Timms, A. W. Promotion of Sandmeyer hydroxylation (homolytic hydroxydediazonation) and hydrodediazonation by chelation of the copper catalyst: bidentate ligands. *Org. Biomol. Chem.* **2**, 1838–1855 (2004).

8. Fattahi, A., Lis, L. & Kass, S. R. Phenylcyclopropane energetics and characterization of its conjugate base: phenyl substituent effects and the C–H bond dissociation energy of cyclopropane. *J. Org. Chem.* **81**, 9175–9179 (2016).
9. Luo, Y.-R. *Handbook of Bond Dissociation Energies in Organic Compounds* (CRC Press, 2003).
10. Cui, X. & Zhang, X. P. in *Contemporary Carbene Chemistry* (eds Moss, R. A. & Doyle, M. P.) 491–525 (Wiley, 2014).
11. Crisenza, G. E. M., Mazzarella, D. & Melchiorre, P. Synthetic methods driven by the photoactivity of electron donor–acceptor complexes. *J. Am. Chem. Soc.* **142**, 5461–5476 (2020).
12. Chemler, S. R., Karyakarte, S. D. & Khoder, Z. M. Stereoselective and regioselective synthesis of heterocycles via copper-catalyzed additions of amine derivatives and alcohols to alkenes. *J. Org. Chem.* **82**, 11311–11325 (2017).
13. Lipp, A., Badir, S. O. & Molander, G. A. Stereoinduction in metallaphotoredox catalysis. *Angew. Chem. Int. Ed.* **60**, 1714–1726 (2021).
14. Prier, C. K., Rankic, D. A. & MacMillan, D. W. C. Visible light photoredox catalysis with transition metal complexes: applications in organic synthesis. *Chem. Rev.* **113**, 5322–5363 (2013).
15. Proctor, R. S. J., Colgan, A. C. & Phipps, R. J. Exploiting attractive non-covalent interactions for the enantioselective catalysis of reactions involving radical intermediates. *Nat. Chem.* **12**, 990–1004 (2020).
16. Skubi, K. L., Blum, T. R. & Yoon, T. P. Dual catalysis strategies in photochemical synthesis. *Chem. Rev.* **116**, 10035–10074 (2016).
17. Zhang, L. & Meggers, E. Steering asymmetric Lewis acid catalysis exclusively with octahedral metal-centered chirality. *Acc. Chem. Res.* **50**, 320–330 (2017).
18. Mondal, S. et al. Enantioselective radical reactions using chiral catalysts. *Chem. Rev.* **122**, 5842–5976 (2022).
19. Li, B., Shi, J.-L. & Xia, Y. Diversified synthesis of all-carbon quaternary *gem*-difluorinated cyclopropanes via copper-catalyzed cross-coupling. *Org. Lett.* **25**, 2674–2679 (2023).
20. McKinney, M. A., Anderson, S. W., Keyes, M. & Schmidt, R. Cyclopropyl halides. Electron transfer in the lithium aluminum hydride reduction of *gem*-dibromo and monobromocyclopropanes. *Tetrahedron Lett.* **23**, 3443–3446 (1982).
21. Tanabe, Y., Wakimura, K.-i & Nishii, Y. Sequential and highly stereoselective intermolecular radical additions of 2,3-*cis*-disubstituted 1,1-dibromo- and 1-bromocyclopropanes to electron-deficient olefins. *Tetrahedron Lett.* **37**, 1837–1840 (1996).
22. Cohen, Y., Cohen, A. & Marek, I. Creating stereocenters within acyclic systems by C–C bond cleavage of cyclopropanes. *Chem. Rev.* **121**, 140–161 (2021).
23. Zhang, Z., Gao, Y., Chen, S. & Wang, J. Transition-metal-catalyzed polymerization of cyclopropenes. *Chin. J. Org. Chem.* **41**, 1888–1896 (2021).
24. Davies, H. M. L. & Liao, K. Dirhodium tetracarboxylates as catalysts for selective intermolecular C–H functionalization. *Nat. Rev. Chem.* **3**, 347–360 (2019).
25. Chen, Y., Fields, K. B. & Zhang, X. P. Bromoporphyrins as versatile synthons for modular construction of chiral porphyrins: cobalt-catalyzed highly enantioselective and diastereoselective cyclopropanation. *J. Am. Chem. Soc.* **126**, 14718–14719 (2004).
26. Zhu, S., Ruppel, J. V., Lu, H., Wojtas, L. & Zhang, X. P. Cobalt-catalyzed asymmetric cyclopropanation with diazosulfones: rigidification and polarization of ligand chiral environment via hydrogen bonding and cyclization. *J. Am. Chem. Soc.* **130**, 5042–5043 (2008).
27. Xu, X. et al. Highly asymmetric intramolecular cyclopropanation of acceptor-substituted diazoacetates by Co(II)-based metalloradical catalysis: iterative approach for development of new-generation catalysts. *J. Am. Chem. Soc.* **133**, 15292–15295 (2011).
28. Hu, Y. et al. Next-generation *D*₂-symmetric chiral porphyrins for cobalt(II)-based metalloradical catalysis: catalyst engineering by distal bridging. *Angew. Chem. Int. Ed.* **58**, 2670–2674 (2019).
29. Ebner, C. & Carreira, E. M. Cyclopropanation strategies in recent total syntheses. *Chem. Rev.* **117**, 11651–11679 (2017).
30. Dian, L. & Marek, I. Asymmetric preparation of polysubstituted cyclopropanes based on direct functionalization of achiral three-membered carbocycles. *Chem. Rev.* **118**, 8415–8434 (2018).
31. Talele, T. T. The ‘cyclopropyl fragment’ is a versatile player that frequently appears in preclinical/clinical drug molecules. *J. Med. Chem.* **59**, 8712–8756 (2016).
32. Top Pharmaceuticals Poster. <https://sites.arizona.edu/njardarson-lab/top200-posters/> (University of Arizona, 2022).
33. Wishart, D. S. et al. DrugBank 5.0: a major update to the DrugBank database for 2018. *Nucleic Acids Res.* **46**, D1074–D1082 (2017).
34. Lebel, H., Marcoux, J.-F., Molinaro, C. & Charette, A. B. Stereoselective cyclopropanation reactions. *Chem. Rev.* **103**, 977–1050 (2003).
35. Mato, M., Franchino, A., Garcia-Morales, C. & Echavarren, A. M. Gold-catalyzed synthesis of small rings. *Chem. Rev.* **121**, 8613–8684 (2021).
36. Kulinkovich, O. G. & de Meijere, A. 1,*n*-Dicarbanionic titanium intermediates from monocarbanionic organometallics and their application in organic synthesis. *Chem. Rev.* **100**, 2789–2834 (2000).
37. Doyle, M. P., Duffy, R., Ratnikov, M. & Zhou, L. Catalytic carbene insertion into C–H bonds. *Chem. Rev.* **110**, 704–724 (2010).
38. He, Y. et al. Recent advances in transition-metal-catalyzed carbene insertion to C–H bonds. *Chem. Soc. Rev.* **51**, 2759–2852 (2022).
39. Wang, X. & Zhang, X. P. in *Transition Metal-Catalyzed Carbene Transformations* (eds Wang, J., Che, C.-M. & Doyle, M. P.) 25–66 (Wiley, 2022).
40. Vicente, R. C–C bond cleavages of cyclopropenes: operating for selective ring-opening reactions. *Chem. Rev.* **121**, 162–226 (2021).
41. Sustac Roman, D. & Charette, A. B. in *C–H Bond Activation and Catalytic Functionalization II* (eds Dixneuf, P. H. & Doucet, H.) 91–114 (Springer, 2015).
42. Shao, Q., Wu, K., Zhuang, Z., Qian, S. & Yu, J.-Q. From Pd(OAc)₂ to chiral catalysts: the discovery and development of bifunctional mono-N-protected amino acid ligands for diverse C–H functionalization reactions. *Acc. Chem. Res.* **53**, 833–851 (2020).
43. Lee, W.-C. C. & Zhang, X. P. Asymmetric radical cyclopropanation of alkenes. *Trends Chem.* **4**, 850–851 (2022).
44. Lee, W.-C. C. & Zhang, X. P. Metalloradical catalysis: general approach for controlling reactivity and selectivity of homolytic radical reactions. *Angew. Chem. Int. Ed.* **63**, e202320243 (2024).
45. Lee, W.-C. C. et al. Asymmetric radical cyclopropanation of dehydroaminocarboxylates: stereoselective synthesis of cyclopropyl α -amino acids. *Chem* **7**, 1588–1601 (2021).
46. Wang, X. et al. Asymmetric radical process for general synthesis of chiral heteroaryl cyclopropanes. *J. Am. Chem. Soc.* **143**, 11121–11129 (2021).
47. Wang, J., Xie, J., Lee, W.-C. C., Wang, D.-S. & Zhang, X. P. Radical differentiation of two ester groups in unsymmetrical diazomalonates for highly asymmetric olefin cyclopropanation. *Chem Catal.* **2**, 330–344 (2022).
48. Ke, J. et al. Metalloradical activation of in situ-generated α -alkynyl diazomethanes for asymmetric radical cyclopropanation of alkenes. *J. Am. Chem. Soc.* **144**, 2368–2378 (2022).
49. Lee, W.-C. C., Wang, D.-S., Zhu, Y. & Zhang, X. P. Iron(III)-based metalloradical catalysis for asymmetric cyclopropanation via a stepwise radical mechanism. *Nat. Chem.* **15**, 1569–1580 (2023).

50. Bhat, V., Welin, E. R., Guo, X. & Stoltz, B. M. Advances in stereoconvergent catalysis from 2005 to 2015: transition-metal-mediated stereoblatant reactions, dynamic kinetic resolutions, and dynamic kinetic asymmetric transformations. *Chem. Rev.* **117**, 4528–4561 (2017).
51. Zhang, X. & Tan, C.-H. Stereospecific and stereoconvergent nucleophilic substitution reactions at tertiary carbon centers. *Chem* **7**, 1451–1486 (2021).
52. An, L., Tong, F.-F., Zhang, S. & Zhang, X. Stereoselective functionalization of racemic cyclopropylzinc reagents via enantiodivergent relay coupling. *J. Am. Chem. Soc.* **142**, 11884–11892 (2020).
53. Müller, D. S. & Marek, I. Copper mediated carbometalation reactions. *Chem. Soc. Rev.* **45**, 4552–4566 (2016).
54. Onneken, C. et al. Light-enabled deracemization of cyclopropanes by Al-salen photocatalysis. *Nature* **621**, 753–759 (2023).
55. Boche, G. & Walborsky, H. M. in *Cyclopropane Derived Reactive Intermediates* (eds Patai, S. & Rappoport, Z.) 117–173 (Wiley, 1990).
56. Gabbey, A. L., Scotchburn, K. & Rousseaux, S. A. L. Metal-catalysed C–C bond formation at cyclopropanes. *Nat. Rev. Chem.* **7**, 548–560 (2023).
57. Rubin, M., Rubina, M. & Gevorgyan, V. Transition metal chemistry of cyclopropenes and cyclopropanes. *Chem. Rev.* **107**, 3117–3179 (2007).
58. Moragas, T. & Martin, R. Nickel-catalyzed reductive carboxylation of cyclopropyl motifs with carbon dioxide. *Synthesis* **48**, 2816–2822 (2016).
59. Mao, R., Balon, J. & Hu, X. Decarboxylative C(sp³)–O cross-coupling. *Angew. Chem. Int. Ed.* **57**, 13624–13628 (2018).
60. Salgueiro, D. C., Chi, B. K., Guzei, I. A., García-Reynaga, P. & Weix, D. J. Control of redox-active ester reactivity enables a general cross-electrophile approach to access arylated strained rings. *Angew. Chem. Int. Ed.* **61**, e202205673 (2022).
61. Chen, T.-G. et al. Building C(sp³)-rich complexity by combining cycloaddition and C–C cross-coupling reactions. *Nature* **560**, 350–354 (2018).
62. West, M. S., Gabbey, A. L., Huestis, M. P. & Rousseaux, S. A. L. Ni-catalyzed reductive cross-coupling of cyclopropylamines and other strained ring NHP esters with (hetero)aryl halides. *Org. Lett.* **24**, 8441–8446 (2022).
63. DeCicco, E. M. et al. Decarboxylative cross-electrophile coupling of (hetero)aromatic bromides and NHP esters. *J. Org. Chem.* **88**, 12329–12340 (2023).
64. Liao, J. et al. Deaminative reductive cross-electrophile couplings of alkylpyridinium salts and aryl bromides. *Org. Lett.* **21**, 2941–2946 (2019).
65. Dong, Z. & MacMillan, D. W. C. Metallaphotoredox-enabled deoxygenative arylation of alcohols. *Nature* **598**, 451–456 (2021).
66. Mills, L. R., Monteith, J. J., dos Passos Gomes, G., Aspuru-Guzik, A. & Rousseaux, S. A. L. The cyclopropane ring as a reporter of radical leaving-group reactivity for Ni-catalyzed C(sp³)–O arylation. *J. Am. Chem. Soc.* **142**, 13246–13254 (2020).
67. Gu, Q.-S., Li, Z.-L. & Liu, X.-Y. Copper(I)-catalyzed asymmetric reactions involving radicals. *Acc. Chem. Res.* **53**, 170–181 (2020).
68. Dong, X.-Y. et al. A general asymmetric copper-catalysed Sonogashira C(sp³)–C(sp) coupling. *Nat. Chem.* **11**, 1158–1166 (2019).
69. Wang, F.-L. et al. Mechanism-based ligand design for copper-catalysed enantioconvergent C(sp³)–C(sp) cross-coupling of tertiary electrophiles with alkynes. *Nat. Chem.* **14**, 949–957 (2022).
70. Wang, L.-L. et al. A general copper-catalysed enantioconvergent radical Michaelis–Becker-type C(sp³)–P cross-coupling. *Nat. Synth.* **2**, 430–438 (2023).
71. Chen, J.-J. et al. Enantioconvergent Cu-catalysed N-alkylation of aliphatic amines. *Nature* **618**, 294–300 (2023).
72. Tian, Y. et al. A general copper-catalysed enantioconvergent C(sp³)–S cross-coupling via biomimetic radical homolytic substitution. *Nat. Chem.* **16**, 466–475 (2024).
73. Ryabchuk, P., Edwards, A., Gerasimchuk, N., Rubina, M. & Rubin, M. Dual control of the selectivity in the formal nucleophilic substitution of bromocyclopropanes en route to densely functionalized, chirally rich cyclopropyl derivatives. *Org. Lett.* **15**, 6010–6013 (2013).
74. Sladojevich, F., Trabocchi, A., Guarna, A. & Dixon, D. J. A new family of cinchona-derived amino phosphine precatalysts: application to the highly enantio- and diastereoselective silver-catalyzed isocyanacetate aldol reaction. *J. Am. Chem. Soc.* **133**, 1710–1713 (2011).
75. Pearson, R. G. Hard and soft acids and bases. *J. Am. Chem. Soc.* **85**, 3533–3539 (1963).
76. Wu, X., Lei, C., Yue, G. & Zhou, J. Palladium-catalyzed direct cyclopropylation of heterocycles. *Angew. Chem. Int. Ed.* **54**, 9601–9605 (2015).
77. Bai, J.-F., Yasumoto, K., Kano, T. & Maruoka, K. Asymmetric synthesis of chiral 1,4-enynes through organocatalytic alkenylation of propargyl alcohols with trialkenylboroxines. *Angew. Chem. Int. Ed.* **58**, 8898–8901 (2019).
78. Xia, H.-D. et al. Photoinduced copper-catalyzed asymmetric decarboxylative alkylation with terminal alkynes. *Angew. Chem. Int. Ed.* **59**, 16926–16932 (2020).
79. Sagadevan, A., Ragupathi, A. & Hwang, K. C. Photoinduced copper-catalyzed regioselective synthesis of indoles: three-component coupling of arylamines, terminal alkynes, and quinones. *Angew. Chem. Int. Ed.* **54**, 13896–13901 (2015).
80. Zhang, Y. et al. Copper-catalyzed photoinduced enantioselective dual carbofunctionalization of alkenes. *Org. Lett.* **22**, 1490–1494 (2020).
81. Harayama, T., Fukushi, H., Ogawa, K. & Yoneda, F. An efficient method for preparing gem-dimethylcyclopropanes from gem-dibromocyclopropanes. *Chem. Pharm. Bull.* **33**, 3564–3566 (1985).
82. Cohen, T., Dietz, A. G. Jr. & Miser, J. R. A simple preparation of phenols from diazonium ions via the generation and oxidation of aryl radicals by copper salts. *J. Org. Chem.* **42**, 2053–2058 (1977).
83. Teator, A. J., Lastovickova, D. N. & Bielawski, C. W. Switchable polymerization catalysts. *Chem. Rev.* **116**, 1969–1992 (2016).
84. Bunschoten, R. P. et al. Mechanistic basis of the Cu(OAc)₂ catalyzed azide–ynamine (3+2) cycloaddition reaction. *J. Am. Chem. Soc.* **146**, 13558–13570 (2024).
85. Chen, S.-J., Krska, S. W. & Stahl, S. S. Copper-catalyzed benzylic C–H cross-coupling enabled by redox buffers: expanding synthetic access to three-dimensional chemical space. *Acc. Chem. Res.* **56**, 3604–3615 (2023).
86. Bakhoda, A. et al. Three-coordinate copper(II) alkynyl complex in C–C bond formation: the sesquicentennial of the Glaser coupling. *J. Am. Chem. Soc.* **142**, 18483–18490 (2020).

Acknowledgements

Financial support from the National Natural Science Foundation of China (numbers 22025103, 92256301 and 22331006 to X.-Y.L.; 22271133 to Q.-S.G.; 22201127 to L.L.), the National Key R&D Program of China (numbers 2021YFF0701604 and 2021YFF0701704, to X.-Y.L.), the Guangdong Innovative Program (number 2019BT02Y335, to X.-Y.L.), the Guangdong Major Project of Basic and Applied Basic Research (number 2023B0303000020, to X.-Y.L.), the New Cornerstone Science Foundation through the Explorer Prize (to X.-Y.L.), the Shenzhen Science and Technology Program

(numbers KQTD20210811090112004, to X.-Y.L. and Q.-S.G.; JCYJ20220818100600001, to X.-Y.L.), the Shenzhen Key Laboratory of Cross-Coupling Reactions (number ZDSYS20220328104200001, to X.-Y.L.), High-Level of Special Funds (number G03050K003, to X.-Y.L.) and the High-Level Key Discipline Construction Project (number G030210001, to X.-Y.L.) is gratefully acknowledged. We appreciate the assistance of SUSTech Core Research Facilities.

Author contributions

Z.G., L.L., W.W. and L.T. designed the experiments and analysed the data. Z.G., L.L., W.W. and N.-Y.Y. performed the experiments. J.-R.L. designed and performed the DFT calculations. L.L., Z.-L.L., Q.-S.G. and X.-Y.L. wrote the paper. Q.-S.G. and X.-Y.L. conceived and supervised the project.

Competing interests

The authors declare no competing interests.

Additional information

Supplementary information The online version contains supplementary material available at <https://doi.org/10.1038/s44160-024-00654-x>.

Correspondence and requests for materials should be addressed to Qiang-Shuai Gu or Xin-Yuan Liu.

Peer review information *Nature Synthesis* thanks the anonymous reviewers for their contribution to the peer review of this work. Primary Handling Editor: Thomas West, in collaboration with the *Nature Synthesis* team.

Reprints and permissions information is available at www.nature.com/reprints.

Publisher's note Springer Nature remains neutral with regard to jurisdictional claims in published maps and institutional affiliations.

Springer Nature or its licensor (e.g. a society or other partner) holds exclusive rights to this article under a publishing agreement with the author(s) or other rightsholder(s); author self-archiving of the accepted manuscript version of this article is solely governed by the terms of such publishing agreement and applicable law.

© The Author(s), under exclusive licence to Springer Nature Limited 2024